

0 0 0 0 4 7 0 7 9 9 1

Presented at the Review - Workshop on the  
National Institute of Dental Research of the  
Department of HEW, Bethesda, MD,  
January 24 - 26, 1977

LBL-6028

c.1

FUNDAMENTALS OF WETTING AND  
BONDING BETWEEN CERAMICS AND METALS

Joseph A. Pask

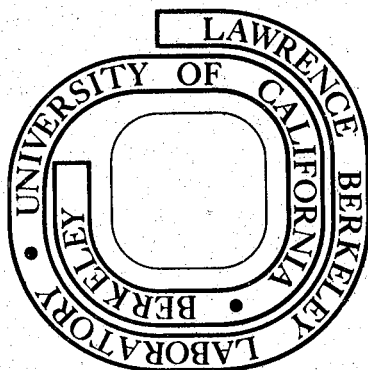
January 21, 1977

RECEIVED  
LIBRARY  
JAN 23 1977  
DOCUMENTS SECTION

Prepared for the U. S. Energy Research and  
Development Administration under Contract W-7405-ENG-48

**For Reference**

Not to be taken from this room



LBL-6028

c.1

**LEGAL NOTICE**

*This report was prepared as an account of work sponsored by the United States Government. Neither the United States nor the United States Energy Research and Development Administration, nor any of their employees, nor any of their contractors, subcontractors, or their employees, makes any warranty, express or implied, or assumes any legal liability or responsibility for the accuracy, completeness or usefulness of any information, apparatus, product or process disclosed, or represents that its use would not infringe privately owned rights.*

FUNDAMENTALS OF WETTING  
AND BONDING BETWEEN CERAMICS AND METALS

Joseph A. Pask

Materials and Molecular Research Division, Lawrence Berkeley Laboratory  
and Department of Materials Science and Mineral Engineering, University  
of California, Berkeley, California 94720

I. INTRODUCTION

Dental porcelains have a substantial amount of an amorphous phase consisting of an alkali aluminosilicate which is a glass at room temperature and becomes a viscous liquid at the temperatures that the porcelain is bonded to a metal. The liquid takes part in the bonding process. The fundamentals associated with fulfilling the requirements for chemical bonding should be the same for all interfaces between dissimilar phases. It is then worthwhile to review and analyze the factors that have been found to be important in the development of adherence or bonding between glass and metal in the fields of porcelain enamels, inorganic protective coatings, and glass-to-metal or ceramic-to-metal seals. Both physical and chemical factors have to be considered.

The most important physical factor in terms of the integrity of the composite is a matching of the thermal expansion characteristics so that the glass is placed under slight compression on cooling from the firing or maturing temperature. This requirement is generally understood and will not be covered in this discussion. It is worthwhile to emphasize, however, the importance of considering the entire thermal expansion curves up to the setting point temperature of the glass and not just up to 300°C, which is the data usually given, in order to obtain a correct indication of the strain that will actually develop at the interface.

This point is illustrated in Fig. 1. It can be seen that if the value at 300°C is used, a differential expansion of 0.00025 unit/unit on cooling is indicated. However, if the value at the setting or solidification point of the glass is taken, the differential expansion is actually only 0.00007 unit/unit which is more acceptable. The actual point of concern in this case is the integrity of the system during cooling since it undergoes a maximum transient expansion differential of 0.00032 unit/unit.

On the other hand, the chemical factors that play a role in developing chemical bonding at the interface are generally not as well understood. The work in our laboratory over many years has resulted in the theory<sup>1</sup> that chemical bonding occurs across the interface when chemical equilibrium relative to the lowest valence oxide of the metallic phase is present, i.e., both the glass and metal at the interface are saturated with the metal oxide and thus the activity of the lowest valence metal oxide is one. Ideally, this condition leads to a monomolecular layer of the metal oxide which is part of the metal and part of the glass. This condition further results in a balance of bond energies and a continuous electronic structure across the interface. This situation is schematically represented in Fig. 2. When the oxide activity is less than one, complete continuity is not realized with the development of van der Waals bonding.

The objective of this paper is to discuss the conditions and the reactions that lead to the realization of chemical equilibrium at interfaces and thus to chemical bonding with specific attention to the platinum/glass and gold/glass systems. Wetting of the solid by the liquid

and the formation of an interface are part of the problem. Sessile drop experiments have been used extensively to generate such information. In many cases, however, the interpretations have been incorrect and misleading. The first part of our detailed discussion will thus deal with this subject.

## II. NATURE OF INTERFACES, WETTING AND SPREADING

An interface is a discontinuity of the bulk structure of a condensed phase. It is called a surface when it is in contact with a gaseous phase. It is called a phase boundary when it is in contact with another condensed phase, amorphous or crystalline. Because of the discontinuity there is always excess free energy at an interface, referred to correspondingly as surface energy or interfacial energy<sup>\*</sup>, over an equivalent portion in the bulk. An interface will form between two condensed phases if its specific free energy is less than the sum of the corresponding specific surface energies ( $\gamma_{sl} < \gamma_{sv} + \gamma_{lv}$ ).

The equilibrium configuration of a sessile drop, expressed in terms of a contact angle between the liquid surface and the solid/liquid interface in a plane perpendicular to the interface and passing through the axis of the drop, is determined by the lowest free energy for the system on the basis of interfacial area considerations assuming that stable or metastable chemical equilibrium exists.<sup>2</sup> If we place a liquid sphere on a flat surface, the initial contact angle is 180°; as an

---

\* Interfacial energy (ergs/cm<sup>2</sup>) and interfacial tension (dynes/cm) will be used interchangeably although they are not exactly equal for a solid;  $\gamma_{sv}$  will refer to the solid/vapor interface,  $\gamma_{sl}$  -- to the solid/liquid interface, and  $\gamma_{lv}$  -- to the liquid/vapor interface.

interface forms, the solid surface area is replaced by an equivalent solid/liquid interface area which increases continuously as the contact angle decreases. There is a corresponding decrease in the liquid surface area, as shown in Fig. 3, as the contact angle decreases to 90° and then an increase as the contact angle continues to decrease to 0°. The free energy changes associated with these changes in the interfacial areas can be represented by

$$\delta G = \delta \int_{sl} (\gamma_{sl} - \gamma_{sv}) dA_{sl} + \delta \int_{lv} \gamma_{lv} dA_{lv} \quad (1)$$

It is possible by use of Eq. (1) to determine whether the contact angle will be acute or obtuse for any combination of relative interfacial tensions as shown in Table 1 which gives the sign of the terms on the right side of the equation. A net negative  $\delta G$  indicates that the formation of the solid/liquid interface has a negative energy and the

Table 1. The Sign of the Terms in Eq. 1 for Possible  $\gamma$  Relationships

$\gamma$ Relationship	First Term	Second Term
For contact angles of 180°→90°		
(a) $\gamma_{sv} < \gamma_{sl} > \gamma_{lv}$	(+)	(-)
(b) $\gamma_{sv} < \gamma_{sl} < \gamma_{lv}$	(+)	(-)
(c) $\gamma_{sv} > \gamma_{sl} > \gamma_{lv}$	(-)	(-)
(d) $\gamma_{sv} > \gamma_{sl} < \gamma_{lv}$	(-)	(-)
For contact angles of 90°→0°		
(a) $\gamma_{sv} < \gamma_{sl} > \gamma_{lv}$	(+)	(+)
(b) $\gamma_{sv} < \gamma_{sl} < \gamma_{lv}$	(+)	(+)
(c) $\gamma_{sv} > \gamma_{sl} > \gamma_{lv}$	(-)	(+)
(d) $\gamma_{sv} > \gamma_{sl} < \gamma_{lv}$	(-)	(+)

contact angle will continue to decrease; the minimum energy configuration

is obtained when  $\delta G$  is zero which is realized when a balance is achieved between the two terms of the equation. It thus can be seen that when  $\gamma_{sv} > \gamma_{sl}$  (cases c and d), the contact angle is always acute; and when  $\gamma_{sv} < \gamma_{sl}$  (cases a and b), the contact angle is always obtuse.

Under stable or metastable equilibrium conditions (absence of a chemical reaction) the actual value of  $\gamma_{sl}$  will always be inbetween the two surface energies and will approach the smaller one as a chemical bond or electronic structure across the interface develops; with van der Waals bonding, the interfacial energy approaches the larger surface energy. In glass/metal systems the contact angle  $\theta$  of the liquid glass on the metal substrate is acute because the surface energy of the glass is less than that of the metal (case c). Surface energies for silicate types of glasses do not vary a great deal and are in the range of about 250 to about 400 ergs/cm<sup>2</sup>. The surface energies of metals are always greater than those of the glasses and are in the range of approximately 1000 to 1800 ergs/cm<sup>2</sup>. The acute angle is the result of wetting of the solid by the liquid, i.e. surface energy of the metal in contact with the liquid glass ( $\gamma_{sl}$ ) is less than the surface energy of the metal in contact with the vapor ( $\gamma_{sv}$ ). This reduction in surface energy of the solid by the liquid ( $\delta\gamma_s$ ) provides the driving force for wetting; resistance to continued wetting of the liquid drop is the energy necessary to extend the surface of the liquid beyond that necessary for adjustment to the change in shape of the drop. A balance of these energies, as represented by the horizontal components of the equivalent surface tensions at the periphery of the liquid drop, determines the equilibrium contact angle as shown in Fig. 4 and is expressed by

$$\delta\gamma_s = \gamma_{sv} - \gamma_{sl} = \gamma_{lv} \cos \theta \quad (2)$$

which is the familiar Young's equation. As indicated above, variation in the nature of the bonding affects the magnitude of  $\gamma_{sl}$  which in turn affects the contact angle, i.e. with a constant  $\gamma_{sv}$  and  $\gamma_{lv}$  chemical bonding will result in a smaller acute contact angle due to a smaller  $\gamma_{sl}$ .

On the other hand, in systems in which  $\gamma_{lv}$  is greater than  $\gamma_{sv}$  the contact angle is always obtuse since  $\gamma_{sl}$  is inbetween and thus greater than  $\gamma_{sv}$  (case b and Fig. 4B). The solid thus is not wetted by the liquid, but the interface forms because the necessary reduction of the free energy of the system is realized by the reduction of the specific surface energy of the liquid by the solids. A balance of the horizontal components of the forces resulting in equilibrium contact angle is again represented by Eq. 2. Examples of these systems are liquid glass on graphite or liquid metal on glass. In these cases chemical bonding can also occur at the solid/liquid interface under stable chemical equilibrium conditions;  $\gamma_{sl}$  will then approach  $\gamma_{sv}$  and with a constant  $\gamma_{sv}$  and  $\gamma_{lv}$  (interfacial van der Waals bonding conditions)  $\gamma_{sl}$  will increase and approach  $\gamma_{lv}$ ; the contact angle will thus approach 180°.

A balance of the vertical forces acting at the "triple point" (solid, liquid, and vapor in equilibrium) must also be present. The magnitude of the attractive forces between the solid and liquid,  $B_v$  in Fig. 4, is determined by the vertical component of the surface tension of the liquid at the triple point, which does not exceed the bonding force at the interface and normally does not distort the solid. The resultant of the horizontal ( $\gamma_{sv} - \gamma_{sl}$ ) and vertical ( $B_v$ ) forces exerted

by the solid becomes a balancing force, B, equal and opposite to the surface tension force of the liquid at the triple point (Fig. 4).

It should be emphasized that for the cases described up to this point no chemical reactions occur at the interfaces, i.e. stable or metastable equilibrium exists, and there is no spreading of the liquid drop. Therefore, for acute angle configurations of liquid glass on metal the driving force for wetting ( $\delta\gamma_s$ ) does not exceed  $\gamma_{lv}$ ; the maximum reduction of  $\gamma_{sv}$  by the liquid is thus equivalent to  $\gamma_{lv}$ , i.e.  $\gamma_{sl} \geq \gamma_{sv} - \gamma_{lv}$ , but in any case  $\gamma_{sl} \geq \gamma_{lv}$ . Consequently the existence of chemical bonding at the interface does not require a zero contact angle or spreading. Similarly, for obtuse angle configurations of liquid metal on ceramic the maximum reduction of  $\gamma_{lv}$  by the solid is equivalent to  $\gamma_{sv}$ ; i.e.  $\gamma_{sl} \geq \gamma_{lv} - \gamma_{sv}$ , but in any case  $\gamma_{sl} \geq \gamma_{sv}$ . Therefore, the existence of interfacial chemical bonding results in obtuse contact angles approaching  $90^\circ$ ; in many cases  $90^\circ$  has been observed experimentally.

These relationships indicate that the sessile drop configuration is determined by the rigid or solid phase and that the solid/liquid interface is dominated by the phase that has the higher surface energy. In other words, the interfacial energy becomes the reduced higher surface energy due to its being wetted by the phase with the lower surface energy. On the other hand, if neither phase dominates the interface and each surface structure essentially maintains its integrity but has some reduction in energy due to van der Waals attractive forces because of being in contact with the other surface, the interfacial energy is greater than either of the surface energies (case a). A large obtuse

angle then forms. It is an indication that a true interface has not formed and adherence would be almost non-existent.

If the bulk phases are not at chemical equilibrium under the conditions of the experiment a thermodynamic driving force for a chemical reaction exists. If kinetic factors are favorable after an interface forms, the reaction begins at the interface. During the reaction there is a dynamic contribution of the free energy of the reaction, whose magnitude is dependent on the nature and rate of the reaction, to the interfacial energy as expressed by

$$\delta\gamma_s = \gamma_{sv} - (\gamma_{sl} + \delta G_R) = \gamma_{lv} \cos \theta. \quad (2)$$

If  $\delta G_R$  is large enough and since it is negative, the left side of the equation can exceed  $\gamma_{lv}$  and spreading can occur (corresponds to case d). Spreading can thus occur for any system under reaction conditions, whether the contact angles would be acute or obtuse under static conditions. After the reaction is complete, the liquid will retract to form sessile drops whose configuration would be determined by the interfacial energies associated with the modified compositions of the reacted phases.

The significance of such reactions, which generally are associated with spreading, is that equilibrium compositions are formed at the interface immediately which is a necessary criterion for chemical bonding. On the other hand, if the reaction results in the appearance of a compound at the interface, the properties of the system will now be equally dependent on the properties of this new phase and its expansion and epitaxial compatibility with the two primary phases.

## III. NATURE OF REACTIONS AT INTERFACES

If the liquid glass-metal assembly is not in chemical equilibrium relative to the metal low valent oxide, a thermodynamic driving force for a reaction exists. If the conditions are favorable, the reaction starts at the interface and progresses into one or both phases by chemical interdiffusion. The resulting compositions in the interface and the interfacial zone most always are in equilibrium because the reaction rates normally are faster than the diffusion rates. Equilibrium is represented by equal chemical potentials or activities for each oxide in the phases comprising the interface. If the bulk phases are not at equilibrium, diffusion, and consequently the reaction, can continue until the whole system reaches equilibrium compositions; the interfacial compositions remain at equilibrium during this process. Since the development of a chemical bond between the phases requires an equilibrium composition only at the interface, in practice the extent of the reaction is kept at a minimum and restricted to the interfacial zone as much as possible. From a physical viewpoint, however, some extension of the interfacial zone may be desirable for the development of a graded seal effect in order to provide a more gradual transition of properties. The bulk of the interacting phases thus normally remains unchanged.

The various types of reactions that may occur have been under study in our laboratory for many years, and the system which was most extensively studied was iron-sodium disilicate ( $NS_2$ ). This can be considered to be a model system in the sense that the glass is relatively simple composition-wise and the reactions are sufficiently extensive so that they can be followed and analyzed with the currently available analytical

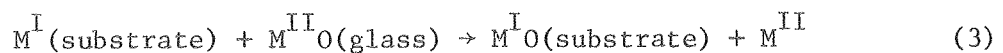
tools. The following discussion is based on these studies and the use of this model for illustrative purposes.<sup>3-6</sup>

The reactions of interest in all cases involve the oxidation of the Fe to form  $\text{Fe}_x\text{O}$  (subsequently referred to as FeO) and the saturation of the interface with FeO. This desired condition can be realized without a reaction by adding the saturation amount of FeO to the  $\text{NS}_2$  glass and sealing it to the unoxidized iron. Development of adherence by this procedure was illustrated by making a series of glasses with increasing amounts of FeO, represented by  $\text{Na}_2\text{Fe}_x\text{Si}_2\text{O}_{5+x}$ . Contact angles decreased from  $60^\circ$  to  $28^\circ$  for glasses whose FeO content increased from 0 to 44 wt% at  $1000^\circ\text{C}$  in a normal vacuum of  $10^{-5}$  torr as shown in the upper curve of Fig. 5.<sup>7,5</sup> The decrease in contact angle is due to a decrease of  $\gamma_{sl}$  as chemical bonding develops;  $\gamma_{sv}$  remains constant and  $\gamma_{lv}$  increases during the series. The adherence increased correspondingly as determined qualitatively by bending the iron platelet; no roughening of the interface was observed indicating that no reaction occurred. This series of glasses is on the join between  $\text{NS}_2$  and FeO in the  $\text{Na}_2\text{O}-\text{SiO}_2-\text{FeO}$  phase equilibrium diagram (Fig. 6); the  $1000^\circ\text{C}$  isotherm crosses this join at 44 wt% FeO, the saturation value. FeO in excess of this value would appear as precipitates in the glass. Use of a bulk glass saturated with the metal oxide is undesirable from several standpoints. In making glass/metal seals the usual procedure is to atmospherically preoxidize the metal substrate to form a desired thickness of oxide coating. The applied glass is then heated to dissolve the oxide coating. Theoretically, a successful seal with good adherence results when the heating is controlled so that essentially a monomolecular layer of metal oxide is

retained at the interface which is chemically bonded to both phases (Fig. 2). Similarly, as long as saturation is maintained an oxide activity of one is maintained across the interface. If after heat treatment a definite oxide layer remains, adherence on the atomic and electronic level should not be affected since the layer is chemically bonded to the substrate metal and the applied glass. A discrete oxide layer, however, can affect the vacuum tightness and strength of the overall system or assembly.

On the other hand, if the heating is continued so that the metal oxide concentration at the interface decreases due to diffusion of the oxide into the bulk of the glass, the activity of the oxide in the glass at the interface decreases. Correspondingly, the continuity of the metal oxide monomolecular layer at the interface is decreased with a decrease in the extent of chemical bonding and a corresponding increase of van der Waals bonding per unit area across the interface and loss of strong adherence. Vacuum tightness, however, normally is not affected. This condition would be similar to that experienced by the glasses with the lower FeO contents in Fig. 5.

Loss of substrate metal oxide layer at the interface results in a potential driving force for a redox reaction involving the oxidation of the substrate metal and the coupled reduction of a cation in the glass indicated by the following general equation where both cations have the same valence.



The significance of this reaction if it occurs is that any metal oxide formed at the interface ( $M^IO$ ) immediately goes into solution in the

adjoining interface glass which tends to maintain the glass at the interface saturated with oxide which is necessary to maintain chemical bonding. The free energy change for this reaction is

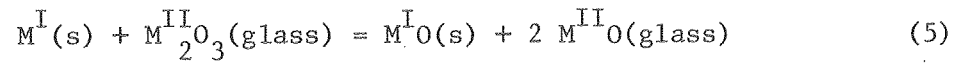
$$\delta G = \delta G^\circ + RT \ln \frac{a(M^I O)_m \cdot a(M^{II})}{a(M^{II} O)_g \cdot a(M^I)} \quad (4)$$

The reaction will occur spontaneously if  $\delta G^\circ$  is negative. If  $\delta G^\circ$  is positive, then the reaction will occur only when the activity quotient (equilibrium constant) is sufficiently less than one to result in an overall negative  $\delta G$ .

The value for  $\delta G^\circ$  is negative when the oxidation potential for the substrate metal,  $M^I$ , is higher than that of the metal for one of the cations in the glass. This basic condition, for example, is attained by the addition of cobalt oxide to porcelain enamels that are applied to iron ( $Fe \rightarrow Fe^{2+}$ , + 0.44;  $Co \rightarrow Co^{2+}$ , + 0.28). When the glass dissolves an existing iron oxide layer and comes into contact with the iron, the reaction represented by Eq. 3 occurs with the formation of dendrites. Since Co and Fe form a complete solid solution, the composition of the dendrite being formed is determined by the amount of iron and cobalt oxide in the adjoining glass. The dendrites growing into the glass have a higher cobalt content due to the decreasing iron oxide gradient into the glass. This gradient creates an electrochemical potential gradient. The electrons released by the iron atoms are transported along the dendrite, or possibly through the glass by a semiconductor mechanism which can be enhanced by manganese oxide additions to the glass, to the precipitating site at the tip of the dendrite where the CoO/FeO ratio is the highest. Cations displaced at the interface by the

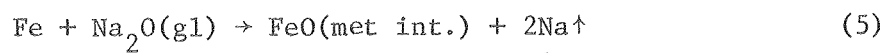
entering iron ions normally  $\text{Na}^+$ , migrate toward the tip of the dendrite where they occupy sites vacated by the reduced cations that are precipitated as atoms. A circuit is thus completed forming a microgalvanic cell. This process continues internally without the need for atmospheric oxidation. Details of such studies have been published.<sup>4</sup> A schematic diagram of the process is shown in Fig. 7. In addition to adding FeO to the glass at the interface the reaction produces a highly irregular interface that contributes to mechanical adherence.

Another redox reaction with a negative  $\delta G^\circ$  that could play a role in introducing the substrate oxide into the glass at the interface can be represented by Eq. (5).



This reaction would be represented by a reduction of ferric ions in the glass to ferrous ions by substrate iron which enters the glass as ferrous ions.

The value for  $\delta G^\circ$  is positive when the oxidation potential for  $\text{M}^{\text{I}}$  is lower than that of all the metals present as cations in the glass. The occurrence of the Eq. 3 reaction is then dependent on the activity quotient of Eq. 4 being sufficiently less than one. This requirement is realized when the glass contains alkali ions and the partial pressure of oxygen ( $P_{\text{O}_2}$ ) in the ambient atmosphere is less than the dissociation pressure for the substrate oxide (FeO in this case). The specific equations are:



$$\delta G = \delta G^\circ + RT \ln \frac{a(\text{FeO})_{\text{int}} \cdot (P_{\text{Na}})^2}{a(\text{Fe}) \cdot a(\text{Na}_2\text{O})_{\text{gl}}} \quad (6)$$

Sessile drop experiments of  $\text{NS}_2$  glass with increasing amounts of FeO on Fe were made at  $1000^\circ\text{C}$  in two furnaces: furnace I - total pressure of  $10^{-8}$  atm and an estimated  $P_{\text{O}_2}$  of about  $10^{-22}$  atm, and furnace II - total pressure of  $7 \times 10^{-8}$  atm and an estimated  $P_{\text{O}_2}$  of about  $1 \times 10^{-8}$  atm. Experiments in furnace II indicate a decreasing contact angle and no reactions as shown by the upper curve in Fig. 5 which was discussed earlier. Experiments in furnace I, however, show that glasses with FeO contents greater than about 9 wt% react with the metal forming Na vapor which deposited in colder portions of the furnace; with the occurrence of the reaction spreading occurred. The spreading was due to the  $\delta G_{\text{R}}$  contribution to the  $\gamma_{\text{s1}}$ ; this caused a sufficient increase of  $\delta\gamma_{\text{s}}$  to exceed  $\gamma_{\text{lv}}$ . Since the total ambient pressure was essentially the same in both furnaces, the critical factor in furnace I was the  $P_{\text{O}_2}$  of about  $10^{-22}$  atm. which was less than the dissociation pressure of  $1.5 \times 10^{-15}$  atm for FeO at  $1000^\circ\text{C}$ . The activity of FeO in the metal interface was thus less than one in furnace I and equal to one in furnace II. A key factor was also the vaporization of Na which occurred because it was reduced by the oxidation of Fe in furnace I and because its boiling point is  $880^\circ\text{C}$ . The net effect of these two factors is to reduce the value of the numerator in the activity quotient in Eq. (6) enough to make the second term of the equation sufficiently large enough to make  $\delta G$  for the reaction negative.

Another point of interest from the reaction viewpoint is that the reaction in furnace I involves replacement of  $2\text{Na}^+$  in the glass by  $\text{Fe}^{2+}$ . The change in composition can then be represented by  $\text{Na}_{2-2x}\text{Fe}_x\text{Si}_2\text{O}_5$ . With increase of Fe the composition change follows the line from  $\text{NS}_2$  in

in Fig. 6 approximately parallel to the  $\text{Na}_2\text{O}$ - $\text{FeO}$  join of the composition triangle until precipitates of  $\text{SiO}_2$  appear in the glass. More detailed experiments of this type as well as for cobalt and nickel with  $\text{NS}_2$  have been described.<sup>5,6</sup>

#### IV. PLATINUM- AND GOLD-CERAMIC SYSTEMS

Many sessile drop experiments of glasses on platinum (Pt) and gold (Au) have been made through the years. The fundamentals that have already been discussed should be applied to the analysis of these systems as well but it has been difficult to do so because of the difficulties of analyzing compositions of thin layers on surfaces and interfaces. This problem exists because of the lack of stability of the bulk metallic oxides at the sealing temperatures and the extremely low solubility of these oxides in the glasses. Interpretations of limited data are thus based on concepts of interface compositions and structures existing at the time. The fairly recent availability of LEED and Auger spectroscopy to analyze surfaces has provided data on Pt and Au surfaces that have led to realistic analyses of sessile drop data.<sup>8,9</sup>

##### 1. Platinum

Sessile drop data for  $B_2O_3$  glass on Pt with increasing ambient pressures at constant temperatures of 700 to 1000°C are shown in Fig. 8.<sup>8</sup> It has been determined that the drop in contact angle from 68° to 6° at a fixed critical pressure for a given test temperature was due to the oxidation of adsorbed carbon on Pt whose removal caused an increase of  $\gamma_{sv}$  and thus an increase in  $\delta\gamma_s$  for wetting. A constant contact angle with continued increase of ambient pressures indicated either no or no further increase of oxygen adsorption. The carbon contamination was caused by emitted organic vapors from parts of the assembly coupled with some backstreaming from the diffusion pump at even the lowest experimental ambient pressures. With proper precautions and design to obtain

carbon-free conditions, the contact angle was invariant at  $\sim 6^\circ$  at all pressures and temperatures.

This analysis is verified by recent studies of adsorption of oxygen and carbon on Pt surfaces.<sup>10</sup> No oxygen adsorption was detected on the low index planes but there was chemisorption on the stepped platinum surfaces. Adsorption of CO and hydrocarbons occurred readily on all crystallographic planes. Also, no chemisorption of water vapor was detected on Pt surfaces by Auger spectroscopy.

Borate glass spread on Pt substrates in sessile drop experiments only when conducted in humid atmospheric air. The spreading indicated that an interfacial chemical reaction had contributed to the lowering of  $\gamma_{sl}$ , i.e.,  $\delta\gamma_s = \gamma_{sv} - (\gamma_{sl} + \delta G_R)$ . It is postulated that the reaction occurred between Pt and chemically absorbed water (hydroxyl ions) in the glass. The solution of the formed oxide in the glass after a short time resulted in the saturation of the glass at the interface and development of adherence. No experimental proof of this saturation to date, however, has been possible because of the very low solubility of the oxide in the glass and consequently the absence of measurable concentration profiles into the glass. Poor adherence was observed in the absence of spreading.

## 2. Gold

Sessile drop data for Na-borate glass on Au with increasing partial pressure of oxygen at  $900^\circ\text{C}$  are shown in Fig. 9.<sup>9</sup> In this case the drop in contact angle from  $46^\circ$  to  $6^\circ$  at a  $P_{\text{O}_2}$  of about  $10^{-2}$  torr ( $10^{-8}$  atm,  $15\mu\text{m Hg}$ ) was presumed to be due to the growth of an oxide layer of some unknown but steady state thickness. The procedure consisted of first

obtaining the contact angle of  $46^\circ$  in vacuum and then introducing oxygen; the time to reach  $6^\circ$  decreased with increase of  $P_{O_2}$ . With the decrease in angle the drop was also observed to move to the edge of the platelet leaving behind a thin film of glass. The movement is postulated to be due to a driving force for solution of the gold oxide; good adherence develops as indicated by fracturing of the glass on bending of the gold piece without detachment of the fractured glass as seen in Fig. 10. This phenomenon and adherence were not observed in vacuum, nitrogen, water vapor, or after exposure to carbon in vacuum at  $900^\circ\text{C}$  for 24 hrs; all of these after some time of exposure show a contact angle of  $46^\circ$ .

Auger analysis showed that oxygen adsorbed strongly on gold and that a small oxygen signal appeared at a  $P_{O_2}$  of  $6 \times 10^{-7}$  torr at  $500^\circ\text{C}$  which could not be removed after heating at  $800^\circ\text{C}$  for 12 hrs in vacuum<sup>11</sup> even though bulk gold oxide begins to decompose at temperatures above about  $140^\circ\text{C}$ . A comparison of these observations with the wetting data suggests that the oxide layer structure changes at a  $P_{O_2}$  of about  $10^{-2}$  torr to make it more reactive. Auger analysis also indicated the appearance of an oxide layer upon treatment of the gold in water vapor under identical conditions.<sup>11</sup> Sessile drop experiments, however, suggest that the oxide layer structure does not change at higher pressure of water vapor as it does at higher  $P_{O_2}$  since no decrease of contact angle to  $6^\circ$  occurs. Auger analysis also showed limited adsorption of carbon.

To illustrate further the applicability of the theory that chemical bonding is developed with the attainment of a metal oxide layer at the interface, contact angle versus time data was obtained for molten gold

on heat-treated and water-soaked sapphire ( $\text{Al}_2\text{O}_3$ ) at  $1100^\circ\text{C}$ .<sup>12</sup> The heat-treated specimen showed a constant angle of  $140^\circ$  after about 3 hr, as expected, because  $\gamma_{1v}$  for molten gold is greater than  $\gamma_{sv}$  for  $\text{Al}_2\text{O}_3$ ; the Au adhered weakly on cooling. The water-soaked  $\text{Al}_2\text{O}_3$  specimen showed an angle of  $125^\circ$ , and the Au adhered strongly. In the latter case, it is postulated that the Au reacted with a hydroxylated  $\text{Al}_2\text{O}_3$  layer when the interface was formed, to form a gold oxide layer at the interface contiguous with both bulk phases. Although bulk gold oxide is unstable at these temperatures, the oxide could persist as a "layer" at the interfacial zone, essentially in equilibrium with both phases, to provide the chemical bonding mechanism. The formation of such a layer is not possible on heat-treated  $\text{Al}_2\text{O}_3$  because of the absence of a hydroxylated layer.

## V. CONCLUSIONS

All of the experimental evidence supports the theory that chemical bonding or strong adherence at an interface between a metal and a ceramic develops when equilibrium compositions relative to the low valent oxide of the metal are present which results in a continuous electronic structure across the interface. This condition develops albeit a discontinuity in bulk atomic structures exists. The theory for bonding has the equivalent statement that the interface should be saturated with the oxide of the substrate, i.e., the activity of substrate oxide is one in both phases. This condition is further equivalent to having a monomolecular layer of the metal oxide which is compatible with and chemically bonds to each of the phases.

If the adjoining phases are at stable or metastable chemical equilibrium, the contact angle in a sessile drop experiment will be acute if  $\gamma_{sv} > \gamma_{lv}$  or obtuse if  $\gamma_{lv} > \gamma_{sv}$ ; no spreading will occur. If the adjoining phases are not at chemical equilibrium, a thermodynamic driving force for a potential reaction exists. The reactions are solution reactions if the metal has been preoxidized. When the liquid glass forms an interface, redox reactions becomes possible. If the contribution of  $\delta G_R$  is sufficiently large, spreading will occur. All of these reactions introduce metal oxide into the glass at the interface tending to achieve or maintain the necessary saturation of the interface with the oxide for adherence.

With the occurrence of a reaction the interface becomes extremely irregular and physically rough since the reaction occurs more extensively at exposed grain boundaries. Reactions which produce dendrites

contribute even more to the irregularity of the interfacial zone. These observations have resulted in proposals that the function of the reactions is to produce an irregular interface which is responsible for the resulting adherence due to an interlocking effect. There is no question that an irregular interface contributes to the mechanical strength of the system. Maximum adherence strength at the interface, however, is dependent upon the presence of chemical bonding.

The interpretation of sessile drop experiments of glass on Pt and Au is based on the same fundamentals, but their interpretation and application becomes difficult because surface compositions and reaction products are sufficiently limited in thickness and amount to present problems of identification. Although they are both "noble" metals, there behavior is not the same. Carbon is an ubiquitous contaminant of Pt, and oxygen is an ubiquitous contaminant of Au. Pt developed a chemical bond to glass by a redox reaction with glass containing dissolved water vapor. Au developed a chemical bond due to solution of an oxide layer by the applied glass.

The same fundamentals and requirements apply to the development of chemical bonding and adherence of metals and their alloys to dental porcelain. The principal problems from a research viewpoint are the experimental identification of the interfacial structures and reactions.

REFERENCES

1. J. A. Pask and R. M. Fulrath, "Fundamentals of Glass-to-Metal Bonding: VIII, J. Am. Ceram. Soc., 45 [12] 592-96 (1962).
2. I. A. Aksay, C. E. Hoge and J. A. Pask, "Wetting Under Chemical Equilibrium and Nonequilibrium Conditions," J. Phys. Chem. 78 [12] 1178-83 (1974).
3. M. P. Borom and J. A. Pask, "Role of 'Adherence Oxides' in the Development of Chemical Bonding at Glass-Metal Interfaces," J. Amer. Ceram. Soc., 49 [1] 1-6 (1966).
4. M. P. Borom, J. A. Longwell and J. A. Pask, "Reactions Between Metallic Iron and Cobalt-Oxide-Bearing Sodium Disilicate Glass," J. Amer. Ceram. Soc., 50 [2] 61-66 (1967).
5. C. E. Hoge, J. J. Brennan and J. A. Pask, "Interfacial Reactions and Wetting Behavior of Glass-Iron Systems," J. Amer. Ceram. Soc., 56 [2] 51-54 (1973).
6. J. J. Brennan and J. A. Pask, "Effect of Composition on Glass-Metal Interface Reactions and Adherence," J. Amer. Ceram. Soc., 56 [2] 58-62 (1973).
7. R. B. Adams and J. A. Pask, "Fundamentals of Glass-to-Metal Bonding: VII, J. Amer. Ceram. Soc., 44 [9] 430-33 (1961).
8. G. A. Holmquist and J. A. Pask, "Effect of Carbon and Water on Wetting and Reactions of  $B_2O_3$ -Containing Glasses on Platinum," J. Am. Ceram. Soc., 59 [9-10] 384-386 (1976).
9. S. T. Tso and J. A. Pask, "Wetting Behavior of  $B_2O_3$ -Containing Glass on Gold," submitted to J. Amer. Ceram. Soc.

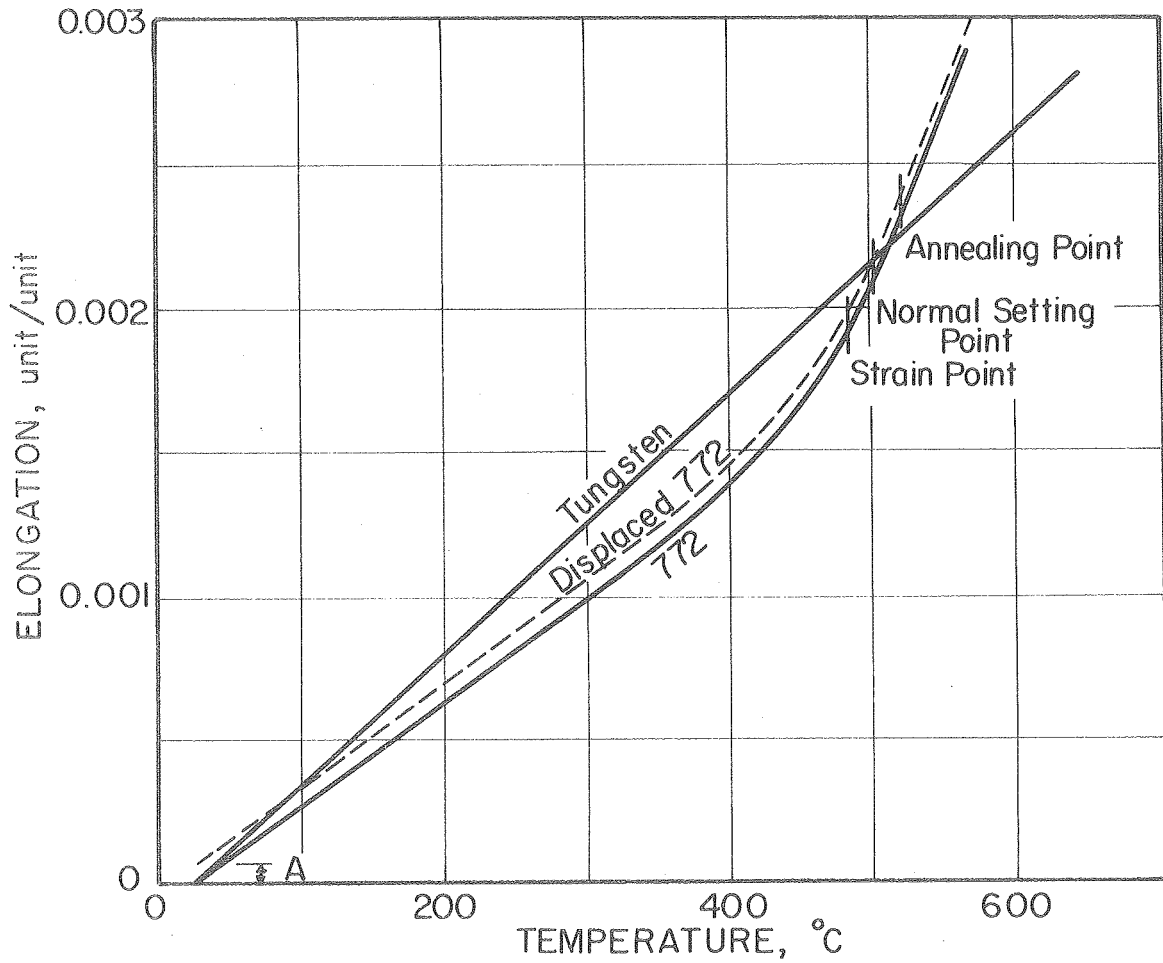
10. B. Lang, R. W. Joyner and G. A. Somorjai, "LEED Studies of Chemisorbed Gases on Stepped Surfaces of Pt," *Surface Sci.*, 30, 454-474 (1972).
11. M. A. Chesters and G. A. Somorjai, "The Chemisorption of Oxygen, Water and Selected Hydrocarbons on the (111) and Stepped Gold Surfaces," *Surface Sci.*, 52, 21-28 (1975).
12. J. J. Brennan and J. A. Pask, "Effect of Nature of Surfaces on Wetting of Sapphire by Liquid Aluminum," *J. Amer. Ceram. Soc.*, 51, [10] 569-573 (1968).

Work performed under the auspices of the U. S. Energy Research and Development Administration.

FIGURES

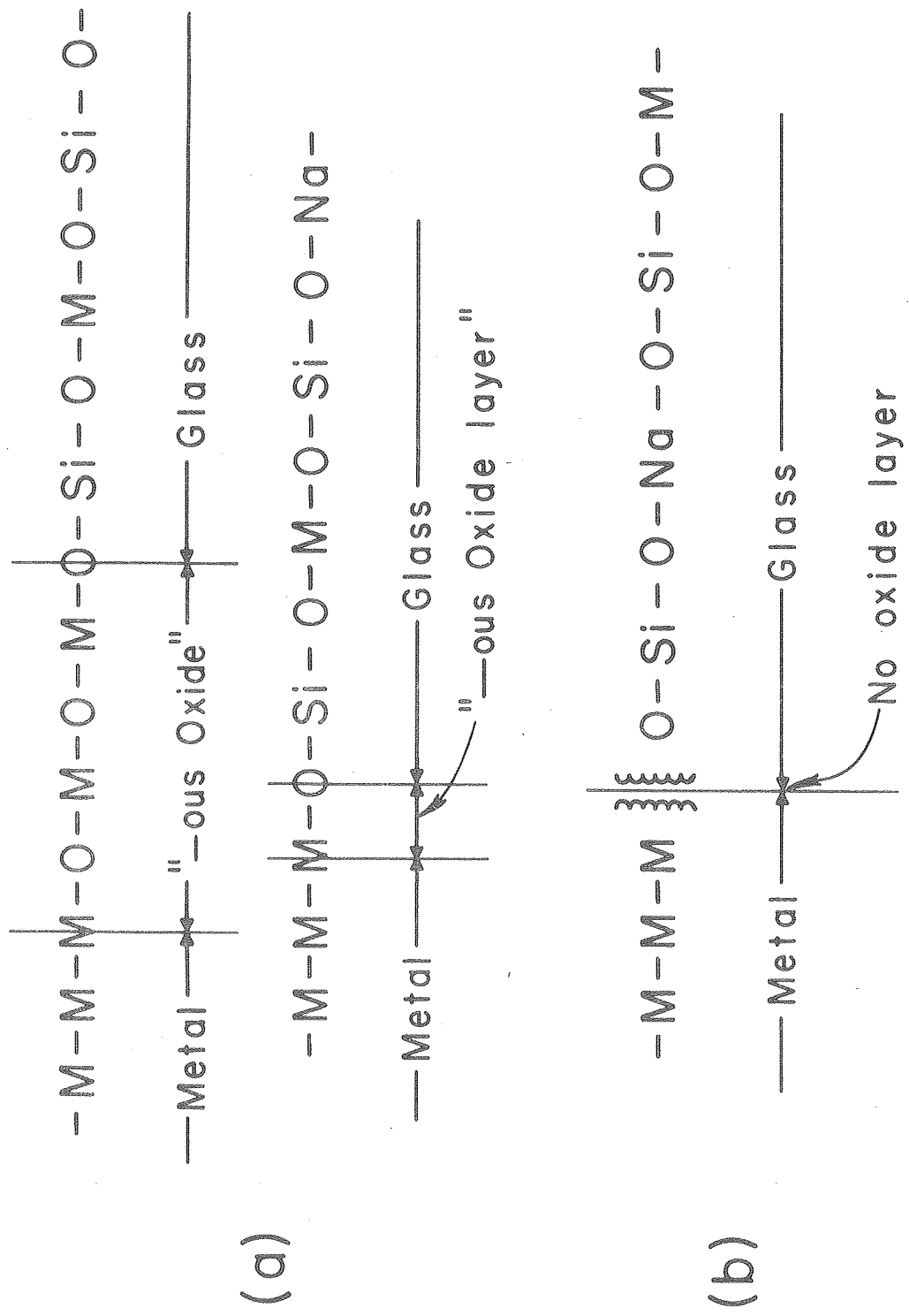
1. To determine differential expansion in a glass-to-metal seal, the glass expansion curve is displaced until the setting point for the conditions of cooling coincides with the metal expansion curve. The spread between these curves then indicates differential expansion, which governs the degree of stress, on cooling. The indicated differential expansion,  $A$ , determines the internal stress in the seal at room temperature.
2. Schematic representing (a) chemical bonding with a discrete oxide layer and an ideal monomolecular layer of oxide, and (b) van der Waals bonding with no oxide layer and an  $a_{\text{FeO}}$  of  $<1$  at the interface.
3. Variation of the solid/liquid and the liquid/vapor interfacial areas vs decreasing contact angle,  $\theta$ , or the height of the drop,  $h$ .  $V_o$  is the volume of the liquid drop.
4. Equilibrium of forces on the periphery of a sessile drop along a vertical plane through the center of the drop for an (a) acute contact angle and (b) obtuse contact angle.  $B$  is the resultant balancing force equal and of opposite direction to  $\gamma_{lv}$  and  $B_v$  is the vertical component equal and of opposite direction to the vertical component of  $\gamma_{lv}$ . The liquid drops are considered to be small enough to neglect gravitational forces.
5. Contact angles of  $\text{Na}_2\text{Si}_2\text{O}_5$  glasses containing increasing amounts of FeO on Fe at  $1000^\circ\text{C}$  in furnace I with  $P_{\text{O}_2} = \sim 10^{-22}$  atm and furnace II with  $P_{\text{O}_2} = \sim 10^{-8}$  atm.

6. Equilibrium phase diagram of the system  $\text{FeO-Na}_2\text{O-SiO}_2$  showing  $1000^\circ\text{C}$  isothermal section and experimental glass compositions.
7. Growth of a dendrite of FeCo composition from the Fe substrate by a microgalvanic cell process.
8. Contact angle vs ambient air pressure for  $\text{B}_2\text{O}_3$  glass on Pt with increasing and decreasing pressures at temperatures indicated under conditions of carbon contamination.
9. Contact angle vs oxygen pressure for sodium borate glass on gold at  $900^\circ\text{C}$ .
10. Adherence of glass to gold indicated by appearance of fracture in the thin glass layer introduced by bending the gold platelet (~128X).



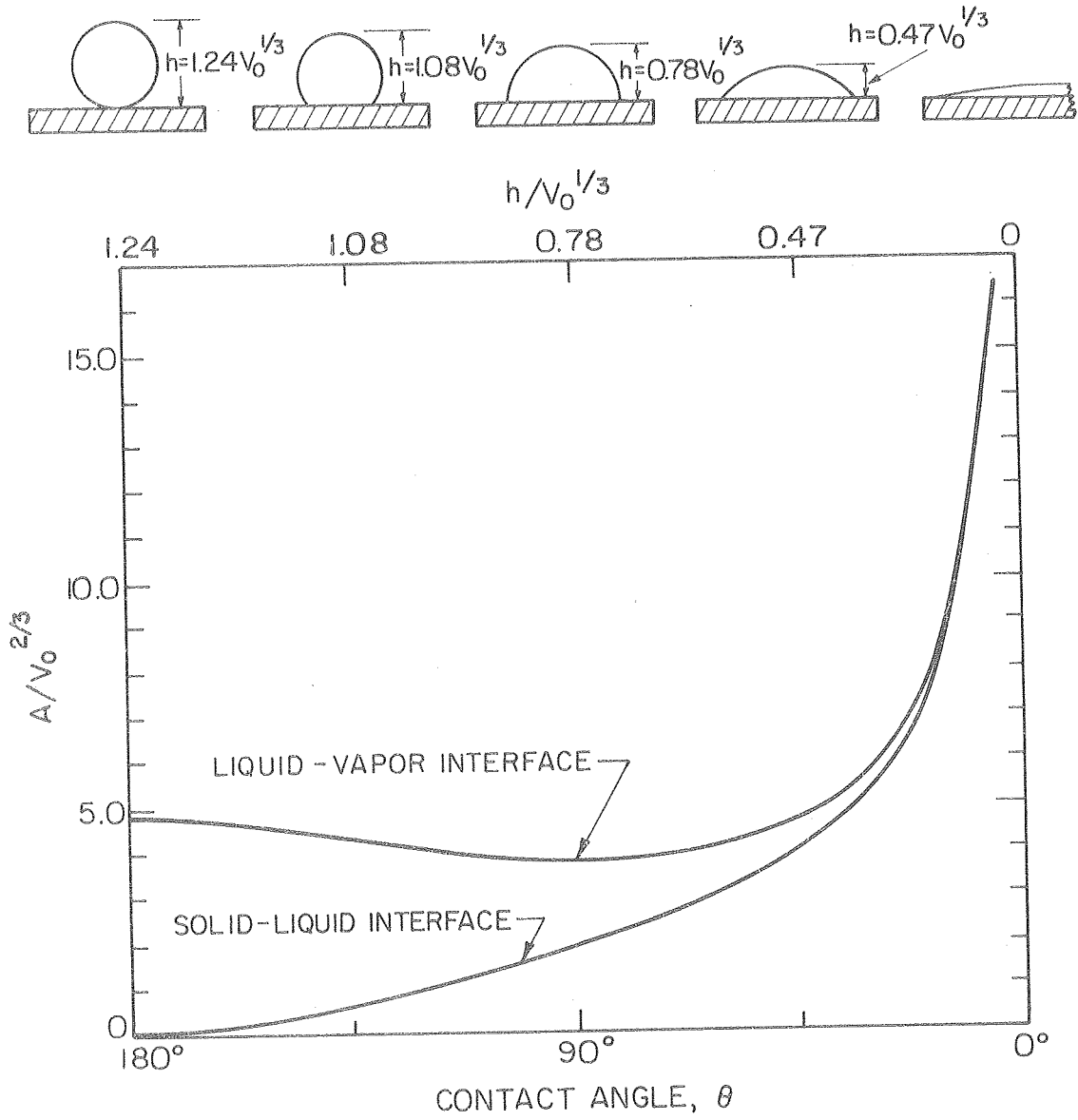
XBL 767-7216

Fig. 1



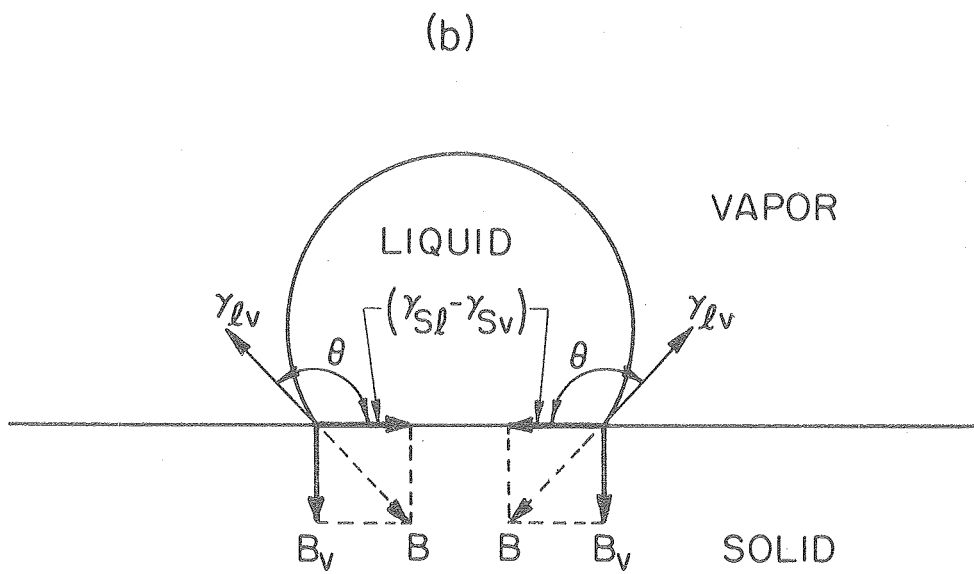
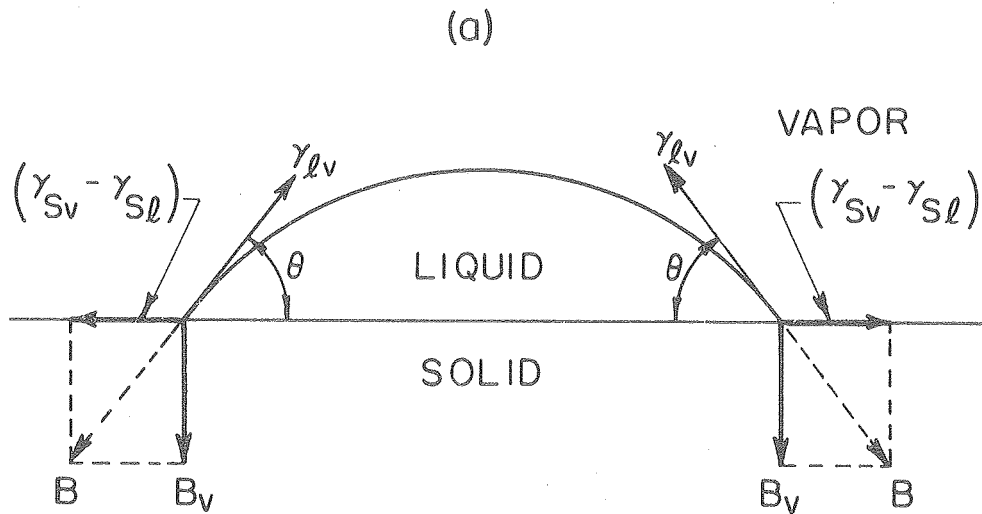
MU-29221

FIG. 2



XBL 738-1701

Fig. 3



XBL 738-1699

Fig. 4

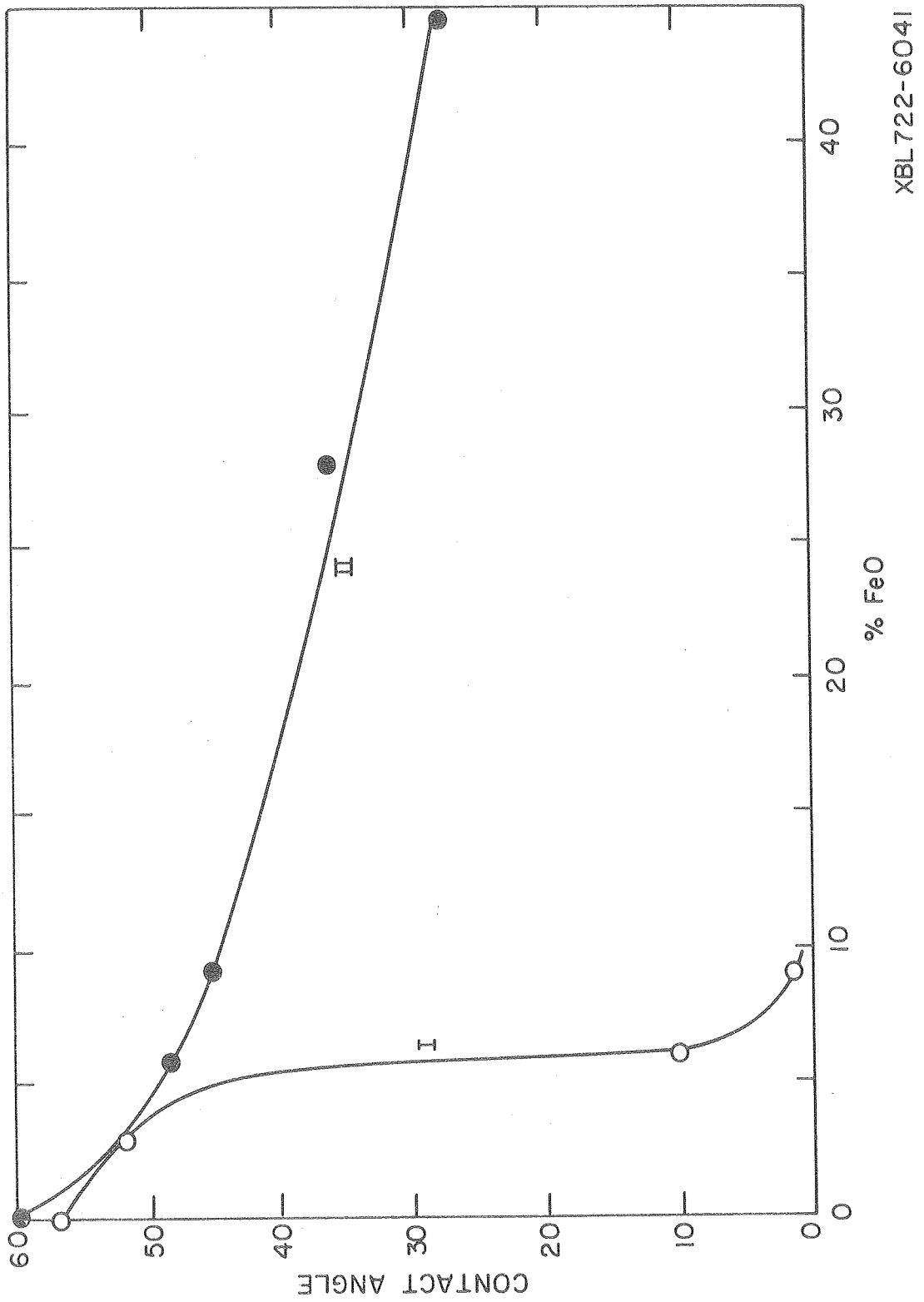


Fig. 5

XBL722-6041

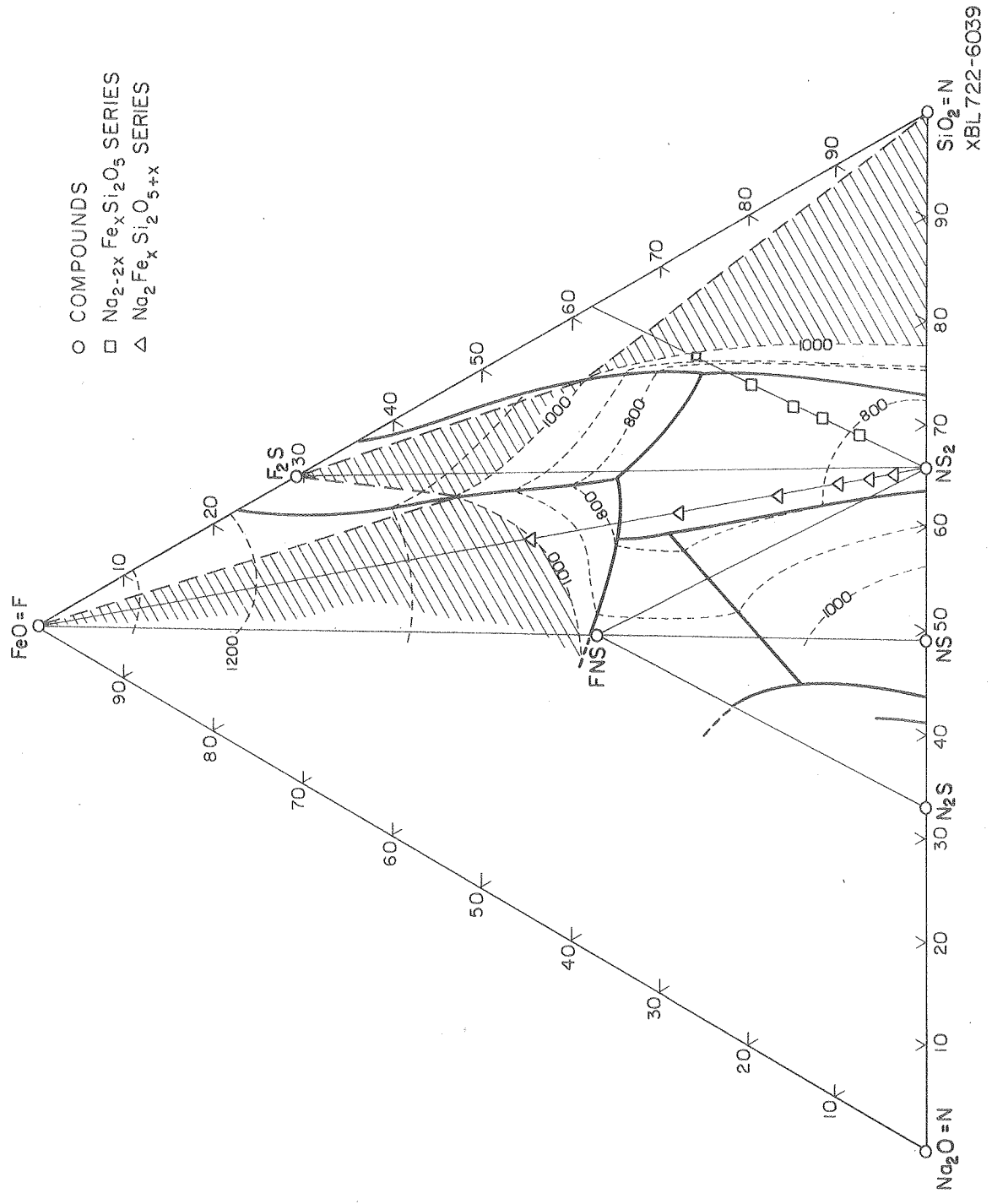
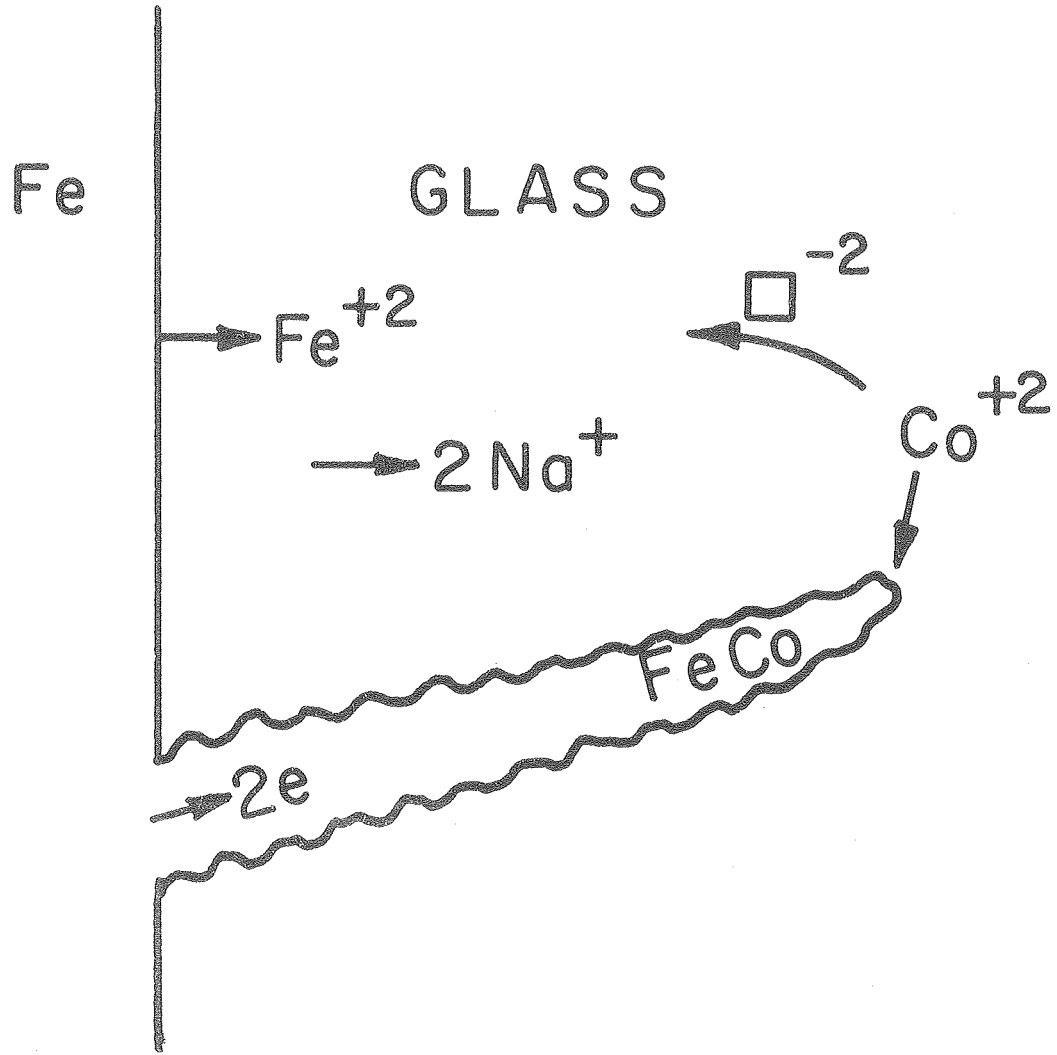
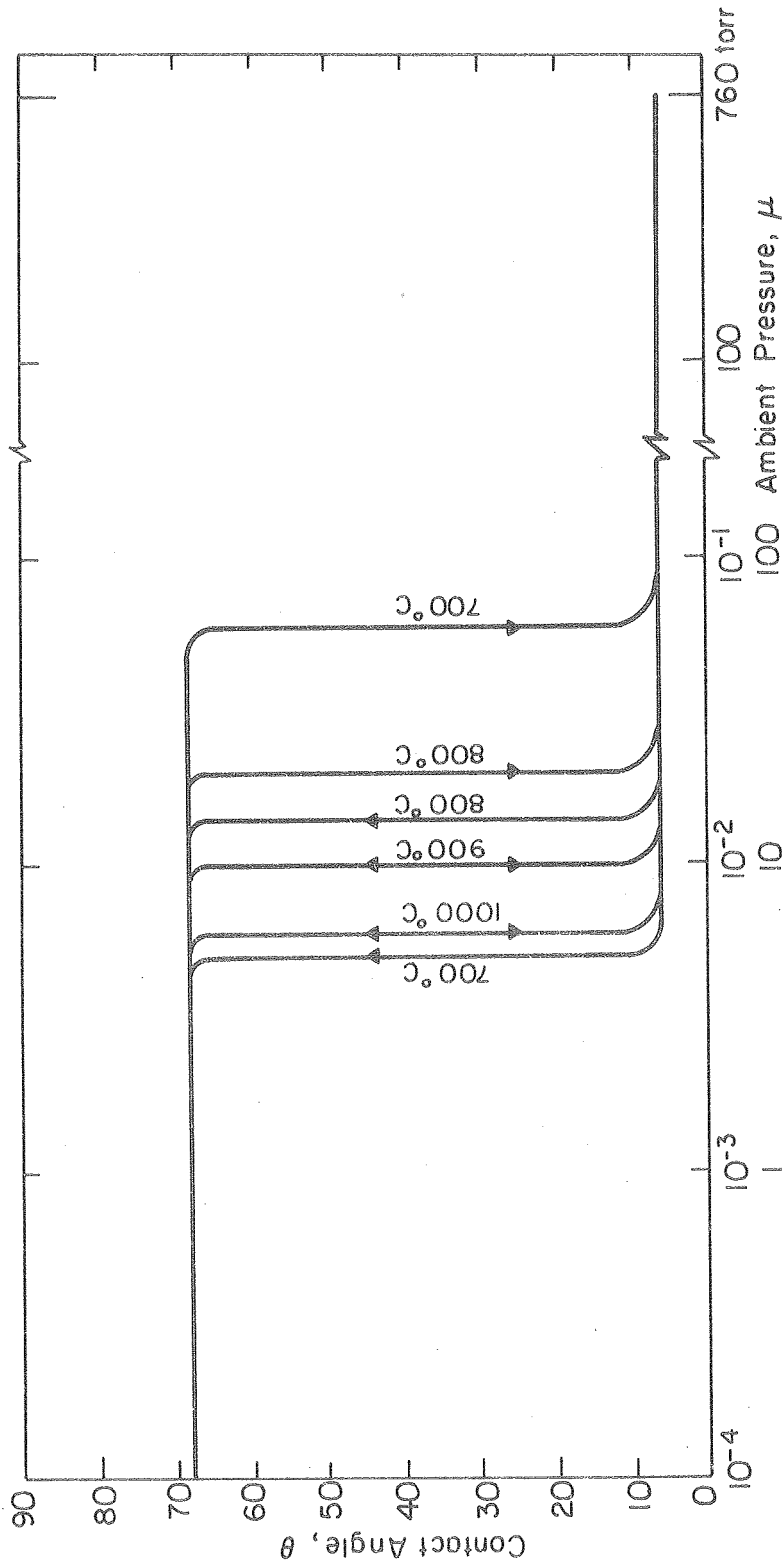


FIG. 6



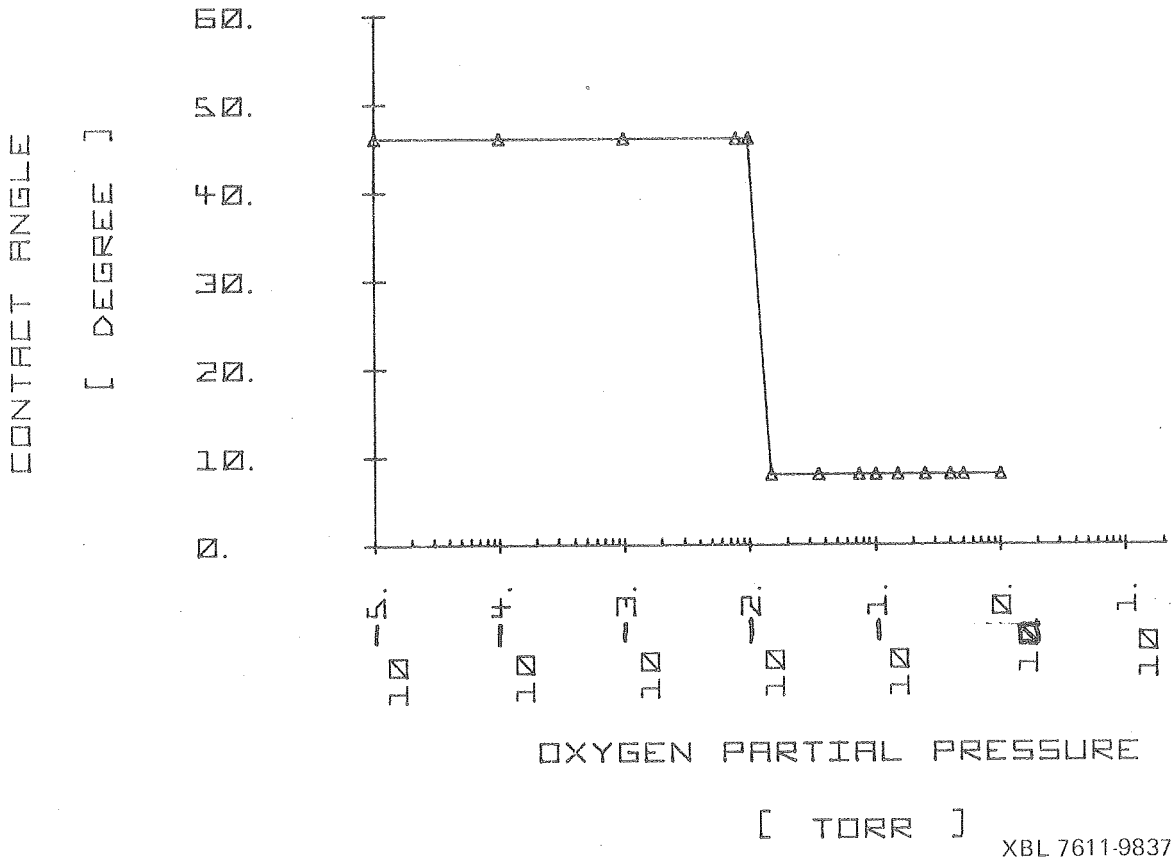
XBL718-7194

Fig. 7



XBL754-6192

Fig. 8



XBL 7611-9837

Fig. 9



Fig. 10

